

# Molecular Structure, HOMO-LUMO, MEP and Fukui Function Analysis of Some TTF-donor Substituted Molecules Using DFT (B3LYP) Calculations

A. Bendjeddou<sup>1\*</sup>, T. Abbaz<sup>1</sup>, A. K. Gouasmia<sup>2</sup> and D. Villemin<sup>3</sup>

<sup>1</sup>Laboratory of Aquatic and Terrestrial Ecosystems, Org. and Bioorg. Chem. Group, University of Mohamed-Cherif Messaadia, Souk Ahras, 41000, Algeria.

<sup>2</sup>Laboratory of Organic Materials and Heterochemistry, University of Larbi Tebessi, Tebessa, 12000, Algeria.

<sup>3</sup>Laboratory of Molecular and Thio-Organic Chemistry, UMR CNRS 6507, INC3M, FR 3038, Labex EMC3, Ensicaen & University of Caen, Caen 14050, France.

## Authors' contributions

This work was carried out in collaboration between all authors. The synthesis part of this work was carried out under the direction of author AKG; the computational study was carried out under the direction of authors DV, TA and AB realized and wrote the work. All authors read and approved the final manuscript.

## Article Information

DOI: 10.9734/IRJPAC/2016/27066

Editor(s):

(1) Wolfgang Linert, Institute of Applied Synthetic Chemistry Vienna University of Technology Getreidemarkt, Austria.

Reviewers:

(1) Alexandre Gonçalves Pinheiro, Ceará State University, Brazil.

(2) M. Rajendran, N M S S Vellaichamy Nadar College, Madurai, Tamilnadu, India.

(3) Tariq Mahmood, COMSATS Institute of Information Technology, University Road, Pakistan.

Complete Peer review History: <http://sciencedomain.org/review-history/15084>

Original Research Article

Received 17<sup>th</sup> May 2016

Accepted 14<sup>th</sup> June 2016

Published 20<sup>th</sup> June 2016

## ABSTRACT

In this letter, through computational study based on density functional theory (DFT/B3LYP) using basis set 6-31G (d,p) a number of global and local reactivity descriptors were computed to predict the reactivity and the reactive sites on the molecules. The molecular geometry and the electronic properties such as frontier molecular orbital (HOMO and LUMO), ionization potential (I) and electron affinity (A) were investigated to get a better insight of the molecular properties. Molecular electrostatic potential (MEP) for all compounds were determined to check their electrophilic or nucleophilic reactivity. The chemometric methods PCA and HCA were employed to find the subset of variables that could correctly classify the compounds according to their reactivity.

\*Corresponding author: E-mail: [amel.bendjeddou@univ-soukahras.dz](mailto:amel.bendjeddou@univ-soukahras.dz);

**Keywords:** Tetrathiafulvalenes; density functional theory; computational chemistry; electronic structure; quantum chemical calculations.

## 1. INTRODUCTION

Heterocyclic compounds are widely distributed in nature and are essential to life in various ways [1]. Since the discovery of organic metals, a large amount of work has been carried out in order to improve the conductivities of salts and charge transfer complexes (CT) of TTF derivatives. However, interest in TTF goes beyond the field of conducting materials. To include its role as an important building block in supramolecular chemistry. Various categories of organic conductors have now been described [2,3], these include systems based upon molecular charge-transfer complexes, conjugated polymers, thiaarene systems and stacked organometallic species, where the metal atoms play no active role in conduction. In the quest to develop these systems various other interesting have come to light. Several kinds of theoretical and experimental work on TTF and its derivatives have been done by a number of workers [4-5] until now.

Reactivity in chemistry is a key concept because it is intimately associated with reaction mechanisms thus allowing understanding chemical reactions and improving synthesis procedures to obtain new materials. A branch of Density Functional Theory (DFT) [6-8] called Conceptual DFT [9-11] has been developed and used in chemistry. As a consequence, a set of global and local descriptors to measure the reactivity of molecular systems has emerged. Due to the diverse biological and industrial importance of tetrathiafulvalenes derivatives a detailed structure-chemical reactivity relations have been undertaken. The present paper gives a complete description of the molecular geometry, global and local reactivity descriptors and MEP features of the title compounds.

## 2. MATERIALS AND METHODS

All computational calculations have been performed on personal computer using the Gaussian 09W program packages developed by Frisch and coworkers [12]. The Becke's three parameter hybrid functional using the LYP correlation functional (B3LYP), one of the most robust functional of the hybrid family, was herein used for all the calculations, with 6.31G (d,p) basis set [13,14]. Gaussian output files were visualized by means of GAUSSIAN VIEW 05

software [15]. Principal component analysis (PCA) [16,17] is a chemometric method was performed using software XLSTAT.

## 3. RESULTS AND DISCUSSION

### 3.1 Chemistry

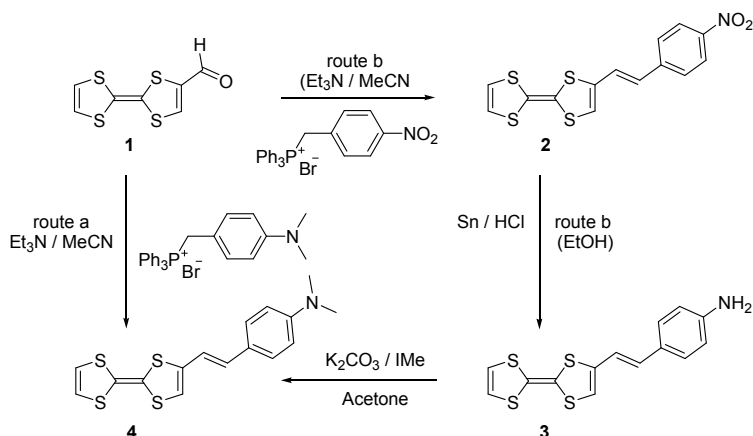
In a previous work [18], we have described the synthesis of TTF-donor substituted molecules **1-4** indicated in Scheme 1. The strategies toward the TTF-vinyl dimethylaniline (TTF-VDMA) **4** are based on Wittig-type condensations between the TTF-carboxaldehyde precursor **1** and an appropriate triphenylphosphonium salt. The more conjugated TTF-VDMA derivative **4** was first synthesized in a multistep sequence (route a) involving, in the first step, the Wittig-type condensation described in the literature. As expected, the reaction between the *p*-nitrobenzyltriphenylphosphonium bromide and TTF-carboxaldehyde in the presence of triethylamine led to **2** in a quite high yield (73%). The nitro compound **2** was then easily converted into **3**, which was finally dialkylated to give the target *N,N*-dimethylated molecule **4** (65%). On the other hand, compound **4** was also obtained in one step in 44% yield through a Wittig condensation between the *p*-dimethylaminobenzyl-triphenylphosphonium bromide and the TTF-carboxaldehyde **1** (route b).

### 3.2 Molecular Geometry

The impact of the geometric structure on the electronic properties manifests itself through the bond lengths and bond angle across the compound backbone, the most relevant structural parameters of title compounds were determined by DFT calculations using B3LYP functional 6-31G (d,p) as basis sets. The geometry of the compounds under investigation is considered by possessing C<sub>1</sub> point group symmetry. The absence of imaginary frequencies confirmed that the stationary points correspond to minima on the Potential Energy Surface. No solvent corrections were made with these calculations. DFT enables to calculate molecular properties such as optimized geometry and energy. Using information obtained as a guide, molecular descriptors calculated using quantum mechanical methods enable determination of

molecular quantities characterizing reactivity, shape and binding properties of molecules. The atoms numbering of molecule used in this paper is reported in Fig. 1. Some selected optimized geometrical parameters of entitled compounds

have been obtained by using the above method and they are presented in Tables 1 and 2. In the present work, geometry optimization parameters for TTF-donor substituted molecules (1-4) have been employed without symmetry constraint.



**Scheme 1. Synthetic route for the preparation of TTF-donor substituted molecules 1-4**

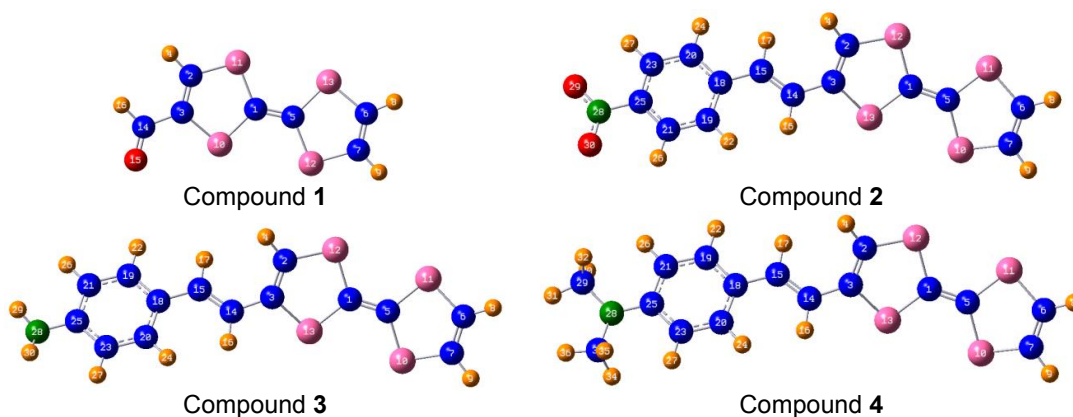


**Fig. 1. Optimized molecular structure of TTF-donor substituted molecules 1-4**

**Table 1. Optimized geometric parameters of compound 1 and 2**

Compound 1				Compound 2			
Bond length (Å)		Bond angles (°)		Bond length (Å)		Bond angles (°)	
R(1,5)	1.350	A(7,6,8)	124.994	R(1,5)	1.350	A(7,6,8)	124.930
R(2,3)	1.351	A(6,7,9)	124.851	R(6,7)	1.337	A(5,10,7)	94.730
R(2,4)	1.085	A(3,2,4)	123.698	R(7,9)	1.083	A(1,12,2)	94.859
R(6,7)	1.337	A(5,1,10)	123.437	R(3,13)	1.787	A(5,1,12)	123.141
R(6,8)	1.083	A(4,2,11)	117.626	R(14,15)	1.351	A(9,7,10)	117.110
R(3,10)	1.773	A(1,5,12)	122.741	R(15,17)	1.088	A(12,1,13)	113.303
R(3,14)	1.463	A(1,11,2)	94.840	R(18,19)	1.412	A(13,3,14)	117.302
R(5,12)	1.786	A(10,3,14)	118.646	R(19,21)	1.387	A(10,5,11)	113.697
R(6,13)	1.763	A(10,1,11)	114.098	R(25,28)	1.467	A(3,14,15)	124.780
R(7,12)	1.762	A(15,14,16)	121.866	R(28,29)	1.232	A(15,18,19)	123.353

Table 2. Optimized geometric parameters of compound 3 and 4

Compound 3				Compound 4			
Bond length (Å)		Bond angles (°)		Bond length (Å)		Bond angles (°)	
R(2,3)	1.349	A(7,6,8)	124.862	R(7,9)	1.083	A(7,6,8)	124.857
R(6,7)	1.337	A(6,7,9)	124.840	R(1,12)	1.785	A(3,2,4)	123.862
R(7,9)	1.083	A(5,1,12)	123.219	R(3,13)	1.789	A(2,3,13)	115.383
R(3,13)	1.789	A(1,5,10)	123.129	R(14,15)	1.352	A(5,1,12)	123.188
R(1,12)	1.785	A(1,12,2)	94.740	R(15,17)	1.090	A(1,5,10)	123.154
R(14,15)	1.352	A(5,11,6)	94.640	R(18,19)	1.407	A(5,10,7)	94.657
R(15,17)	1.090	A(13,3,14)	117.023	R(19,21)	1.387	A(3,14,15)	124.137
R(18,19)	1.408	A(3,14,15)	124.222	R(21,25)	1.414	A(14,15,17)	117.599
R(19,21)	1.388	A(14,15,17)	117.640	R(28,29)	1.453	A(19,18,20)	116.507
R(25,28)	1.390	A(15,18,19)	119.299	R(29,30)	1.096	A(18,19,21)	122.372

### 3.3 Molecular Electrostatic Potential (ESP) Map

Molecular electrostatic potential (ESP) at a point in the space around a molecule gives an indication of the net electrostatic effect produced at that point by the total charge distribution (electron + nuclei) of the molecule and correlates with dipole moments, electro negativity, partial charges and chemical reactivity of the molecule. It provides a visual method to understand the relative polarity of the molecule. The negative electrostatic potential corresponds to an attraction of the proton by the concentrated electron density in the molecule. The positive electrostatic potential corresponds to repulsion of the proton by the atomic nuclei in regions where low electron density exist and the nuclear charge

is incompletely shielded. For all compounds 1-4 were MEP was calculated by DFT/B3LYP at 6-31G (d,p) basis set and MEP surface are plotted in Fig. 2. An electron density is surface mapped with electrostatic potential surface depicts the size, shape, charge density and reactive sites of the molecules [19-21]. The different values of the electrostatic potential represented by different colors; red represents the regions of the most negative electrostatic potential, blue represents the regions of the most positive electrostatic potential and green represents the region of zero potential [22]. Fig. 2 provides a visual representation of the chemically active sites and comparative reactivity of atoms and it is clear that in compounds 1 and 2 oxygen atom (red region) of aldehyde and nitro groups react with electrophilic sites. In all compounds hydrogens atoms (blue region) react with nucleophilic sites.

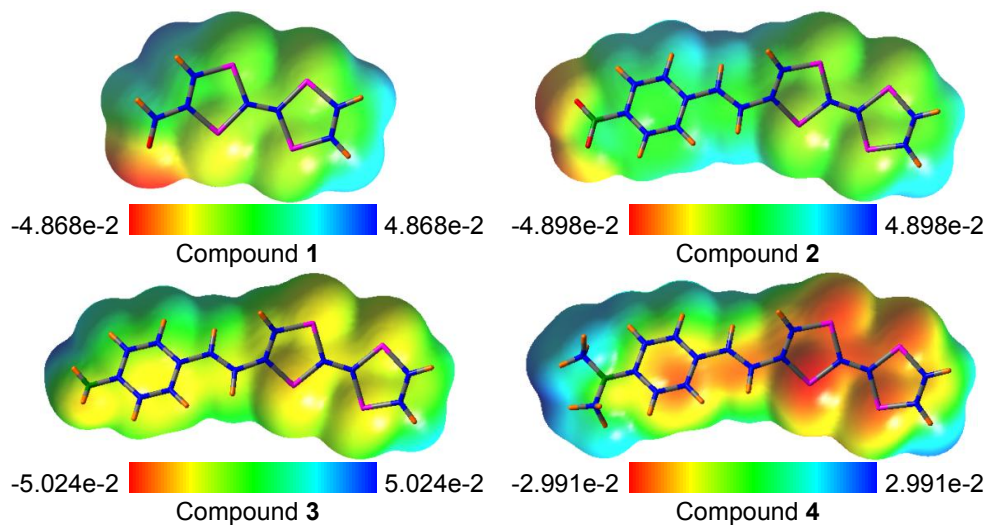


Fig. 2. Molecular electrostatic potential surface of compounds 1-4

### 3.4 Frontier Molecular Orbitals (FMOS)

The frontier molecular orbital determine the way in which the molecule interacts with other species. HOMO (highest occupied molecular orbital), which can be thought the outermost orbital containing electrons, tends to give these electrons such as an electron donor. On the other hand, LUMO (lowest unoccupied molecular orbital) can be thought the innermost orbital containing free places to accept electrons [23]. Therefore, while the energy of the HOMO is directly related to the ionization potential, LUMO energy is directly related to the electron affinity. Energy difference between HOMO and LUMO orbital is called as energy gap that is an important stability for structures [24]. HOMO-LUMO helps to characterize the chemical reactivity and kinetic stability of the molecule [25]. A molecule with a small gap is more polarized and is known as soft molecule. Recently, the energy gap between HOMO and LUMO has been used to prove the bioactivity from intramolecular charge transfer (ICT) [26,27] because it is a measure of electron conductivity. The frontier orbital (HOMO, LUMO) of TTF-donor substituted molecules **1-4**, with B3LYP/6-31G(d,p) method is plotted in Fig. 3. The HOMO and LUMO energy gap of title compounds **1-4** calculated by B3LYP/6-31G(d,p) method are given in Table 3.

### 3.5 Global Reactivity Descriptors

The chemical reactivity of the molecular systems has been determined by the conceptual density functional theory [6]. Electronegativity ( $\chi$ ) chemical potential ( $\mu$ ), global hardness ( $\eta$ ),

global softness ( $S$ ) and electrophilicity index ( $\omega$ ) are global reactivity descriptors, highly successful in predicting global reactivity trends on the basis of Koopmans's theorem, [17] global reactivity descriptors are calculated using the energies of frontier molecular orbitals  $E_{\text{HOMO}}$ ,  $E_{\text{LUMO}}$  as  $\chi = -1/2(E_{\text{LUMO}} + E_{\text{HOMO}})$ ,  $\mu = -\chi = 1/2(E_{\text{LUMO}} + E_{\text{HOMO}})$ ,  $\eta = 1/2(E_{\text{LUMO}} - E_{\text{HOMO}})$ ,  $S = 1/2\eta$  and  $\omega = \mu^2/2\eta$ . The energies of frontier molecular orbitals ( $E_{\text{LUMO}}$ ,  $E_{\text{HOMO}}$ ) and global reactivity descriptors for **1**, **2** are listed in Tables 3 and 4.

The frontier orbital gap helps to characterize molecular electrical transport properties [28,29], the chemical reactivity and kinetic stability of the molecule. A molecule with a small frontier orbital gap is generally associated with a high chemical reactivity and low kinetic stability. The frontier orbital energy gap for both the compounds was found to be 2.891 eV, 2.101 eV, 3.100 eV and 3.120 eV respectively. Larger the HOMO-LUMO energy gap, harder the molecule. The HOMO-LUMO energy gap of compounds **4**, **3** and **1** was slightly larger, signifying higher excitation energy in comparison to **2**, hence compounds **4**, **3** and **1** are harder in comparison to compound **2**. When two molecules react, which one will act as an electrophile or nucleophile will depend upon the value of electrophilicity index. Higher the value of the electrophilicity index better is the electrophilic character. Thus, between all compounds, compound **2** acts as a good electrophile as the molecule shows higher value for global electrophilicity index ( $\omega$ ) at 6.794 eV, as compared to compounds **1**, **3** and **4** whose values for global electrophilicity index ( $\omega$ ) was 4.113 eV, 2.597 eV and 2.466 eV.

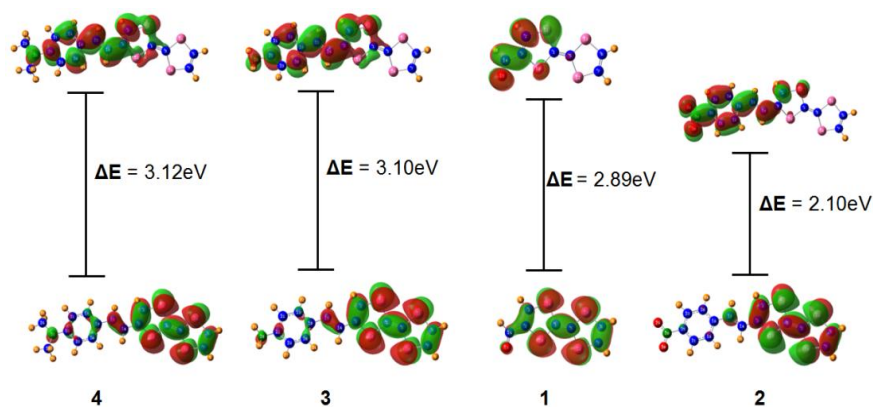


Fig. 3. Highest occupied molecular orbitals and lowest unoccupied molecular orbitals of compounds **1-4**

**Table 3. Energetic parameters of TTF-donor substituted molecules 1-4**

Compounds	E <sub>HOMO</sub> (eV)	E <sub>LUMO</sub> (eV)	ΔE <sub>gap</sub> (eV)	I(eV)	A(eV)
1	-4.894	-2.003	2.891	4.894	2.003
2	-4.828	-2.727	2.101	4.828	2.727
3	-4.388	-1.287	3.100	4.388	1.287
4	-4.334	-1.214	3.120	4.334	1.214

**Table 4. Quantum chemical descriptors of TTF-donor substituted molecules 1-4**

Compounds	μ(eV)	χ(eV)	η(eV)	S(eV)	ω(eV)
1	-3.449	3.449	1.446	0.346	4.113
2	-3.778	3.778	1.050	0.476	6.794
3	-2.838	2.838	1.550	0.323	2.597
4	-2.774	2.774	1.560	0.321	2.466

To analyze the chemical behavior of some substituted TTF, we evaluated their global and local reactivity descriptors. The values of  $\mu$ ,  $\chi$ , S and  $\omega$  were calculated and the results are reported in Table 4. The chemical hardness (softness) value of compound **2** ( $\eta = 1.050$  eV) is lesser (greater) among all the molecules. Thus, compound **2** is found to be more reactive than all the compounds. Also, noted that compound **2** possesses higher electronegativity value ( $\chi = 3.778$  eV) than all compounds so; it is the best electron acceptor. In addition, the value of  $\omega$  for compound **2** ( $\omega = 6.794$  eV) indicates that it is the stronger electrophiles than all compounds. Moreover, compound **2** has the smaller frontier orbital gap so, it is more polarizable and is associated with a high chemical reactivity, low kinetic stability and is also termed as soft molecule.

### 3.6 Local Reactivity Descriptors

The local reactivity descriptor like Fukui function indicates preferred regions where a chemical specie (molecule) will amend its density when numbers of electrons are modified or it indicates tendency of electronic density to deform at a given position upon accepting or donating electrons [30,31]. The condensed or atomic Fukui functions on the  $k^{\text{th}}$  atom site, for electrophilic ( $f_k^-$ ), nucleophilic ( $f_k^+$ ) and free radical ( $f_k^0$ ) attacks are defined as:  $f_k^+ = [q_k(N+1) - q_k(N)]$ ,  $f_k^- = [q_k(N) - q_k(N-1)]$  and  $f_k^0 = [q_k(N+1) - q_k(N-1)]/2$  respectively, where  $q_k$  is atomic charge (Mulliken, Hirschfeld or NBO, etc.) at the  $k^{\text{th}}$  atomic site in the anionic (N+1), cationic (N-1) or neutral molecule. Parr and Yang showed that sites in chemical species with the largest values of Fukui function ( $f_k$ )

shows high reactivity for corresponding attacks. In the title compounds, the order of the reactive sites for electrophilic attack, nucleophilic attack and free radical attacks is given in Tables 5 and 6.

For compounds **1** and **2**, the parameters of local reactivity descriptors show that 1C is the more reactive site for nucleophilic and free radical attacks and 3C, 2C for electrophilic attack. For compounds **3** and **4** the most reactive site for nucleophilic, free radical and electrophilic attack is 1C.

### 3.7 Principal Component Analysis (PCA)

In this work, we auto scaled all calculated variables in order to compare them in the same scale. Afterwards, PCA (principal component analysis) was used to reduce the number of variables and select the most relevant ones, i.e. those responsible for the tetrathiafulvalenes derivatives reactivity. After performing many tests, a good separation is obtained between more active and less active tetrathiafulvalenes compounds using ten variables: I, A,  $\chi$ ,  $\eta$ , s,  $\mu$ ,  $\omega$ , EHOMO, ELUMO,  $\Delta E_{\text{gap}}$  (see Table 3 and 4).

We can observe from PCA results that the first three principal components (PC1, PC2 and PC3) describe 99.71% of the overall variance as follows: PC1 = 93.63%, PC2 = 3.57% and PC3 = 2.51%. The score plot of the variances is a reliable representation of the spatial distribution of the points for the data set studied after explaining almost all of the variances by the first two PCs. The most informative score plot is presented in Fig. 4 (PC1 versus PC2) and we can see that PC1 alone is responsible for the separation between more active **1** and **2** and less active compounds **3** and **4** where PC1 > 0 for the



more active compounds and  $PC1 < 0$  for the less active ones. The same results follow in the case of global reactivity trend based on  $\omega$ .

The loading vectors for the first two principal components (PC1 and PC2) are displayed in Fig. 5. We can see that more active compounds ( $PC1 > 0$ ) can be obtained when we have higher A, I, S,  $\chi$ ,  $\omega$ , values. In this way, some important features on the more active compounds can be observed.

### 3.8 Hierarchical Cluster Analysis (HCA)

Fig. 6 shows HCA analysis of the current study. The horizontal lines represent the compounds and the vertical lines the similarity values between pairs of compounds, a compound and a group of compounds and among groups of compounds. We can note that HCA results are very similar to those obtained with the PCA analysis, i.e. the compounds studied were grouped into two categories: More actives

compounds **1** and **2** and less active compounds **3** and **4**.

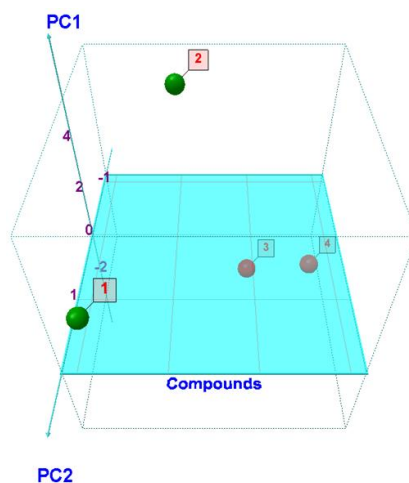


Fig. 4. Score plot for TTF-donor substituted molecules 1-4 in gas phase

Table 5. Order of the reactive sites on compounds 1 and 2

	Compound 1				Compound 2				
Atom	1 C	3 C	7 C	6 C	Atom	1 C	3 C	25 C	30 O
$f^+$	0.059	0.004	0.000	-0.001	$f^+$	0.028	0.021	0.006	0.003
Atom	3 C	5 C	6 C	7 C	Atom	2 C	18 C	1 C	5 C
$f^-$	0.027	0.008	-0.003	-0.003	$f^-$	0.009	0.008	0.005	0.004
Atom	1 C	3 C	7 C	6 C	Atom	1 C	3 C	18 C	7 C
$f^0$	0.026	0.016	-0.001	-0.002	$f^0$	0.017	0.010	0.002	0.000

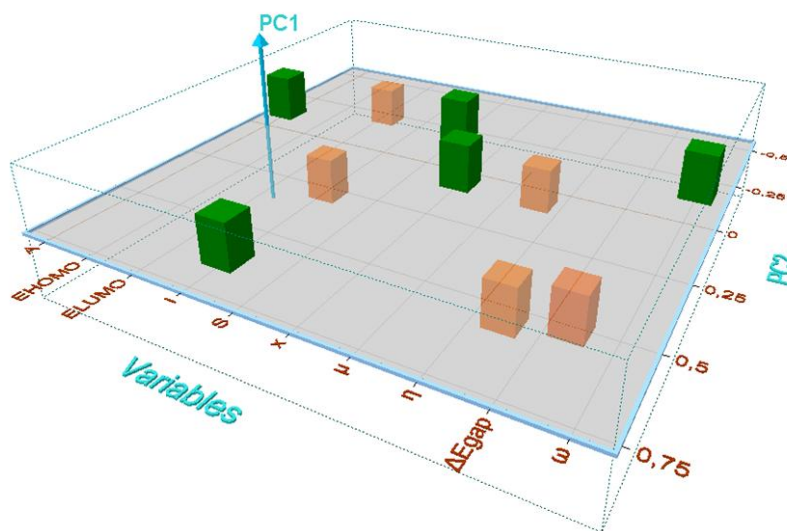
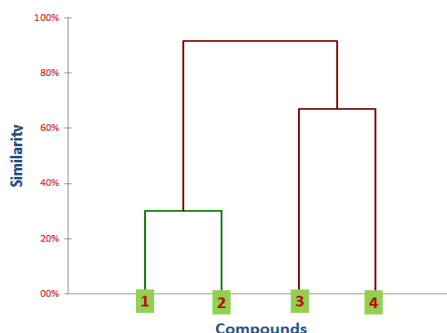


Fig. 5. Loading plot for the variables responsible for the classification of the TTF-donor substituted molecules studied

**Table 6. Order of the reactive sites on compounds 3 and 4**

Compound 3					Compound 4				
Atom	1 C	18 C	21 C	23 C	Atom	1 C	28 N	21 C	20 C
$f^+$	0.036	0.027	0.003	0.003	$f^+$	0.034	0.034	0.032	0.007
Atom	1 C	2 C	18 C	7 C	Atom	1 C	29 C	33 C	23 C
$f^-$	0.020	0.006	0.005	0.000	$f^-$	0.021	0.018	0.018	0.009
Atom	1 C	18 C	23 C	21 C	Atom	1 C	29 C	33 C	20 C
$f^0$	0.028	0.016	0.001	0.001	$f^0$	0.028	0.022	0.021	0.005

**Fig. 6. Dendrogram obtained for TTF-donor substituted molecules studied**

#### 4. CONCLUSION

In conclusion, based on the density functional theory B3LYP/6-31G(d,p) method, The optimized geometric parameters (bond lengths and bond angles) are theoretically determined. The global and local descriptors have been used to investigate the reactivity of different cationic, anionic and radical sites and the influence of these on the molecular interaction in a qualitative and quantitative way. The descriptors obtained could also provide more information and may contribute to a better understanding of the electronic structure of these compounds. The MEP map shows the negative potential sites are on oxygen atoms as well as the positive potential sites around the hydrogen atoms. Compound 2 is more polarizable and is associated with a high chemical reactivity and is also termed as soft molecule. In addition, theoretical results from reactivity descriptors for title compounds show most reactivity at C1 for nucleophilic attack; hence it may be used as a precursor for the synthesis of new heterocyclic compounds such as donors containing TTF moieties. From PCA results, Consistency between the results obtained through the reactivity descriptors and those that determined From PCA analysis. Finally we hope that these consequences will be of assistance in the quest of the experimental and theoretical evidence for the title compound in molecular bindings.

#### COMPETING INTERESTS

Authors have declared that no competing interests exist.

#### REFERENCES

1. Acheson RM. An introduction to the chemistry of heterocyclic compounds. John Wiley, BSP Books New Delhi, India; 2009.
2. Torrance JB. The difference between metallic and insulating salts of tetracyanoquinodimethone (TCNQ): How to design an organic metal. *Acc. Chem. Res.* 1979;12(3):79-86.
3. Bryce MR, Murphy LC. Organic metals. *Nature.* 1984;309:119-126.
4. Mukherjee V, Singh NP. Theoretical vibrational spectra and thermodynamics of organic semiconductive tetrathiafulvalene and its cation radical. *Spectrochimica Acta Part A: Molecular and Biomolecular Spectroscopy.* 2014;117:315-322
5. Shanigaram B, Chitumalla RK, Bhanuprakash K. Adsorption of TCNQ and F4-TCNQ molecules on hydrogen-terminated Si (1 1 1) surface: Van der Waals interactions included DFT study of the molecular orientations. *Computational and Theoretical Chemistry.* 2016;1084: 179-187.
6. Parr RG, Yang W. Density-functional theory of atoms and molecules. Oxford University Press, New York; 1989.
7. Hohenberg P, Kohn W. Inhomogeneous electron gas. *Phys Rev B.* 1964;136:864-871.
8. Kohn W, Sham LJ. Self-Consistent equations including exchange and correlation effects. *Phys. Rev. A.* 1965; 140:1133-1138.
9. Parr RG, Yang W. Density-functional theory of the electronic structure of molecules. *Annu Rev Phys Chem.* 1995; 46:701-728.
10. Ayers P, Parr RG. Variational principles for describing chemical reactions: The Fukui function and chemical hardness revisited. *J Am Chem Soc.* 2000;122(9):2010-2018.



11. Geerlings P, De Proft F, Langenaeker W. Conceptual density functional theory. *Chem. Rev.* 2003;103(5):1793-1874.
12. Frisch MJ, Trucks GW, Schlegel HB, Scuseria GE, Robb MA, Cheeseman JR, Scalmani G, Barone V, Mennucci B, Petersson GA. Gaussian 09, Revision C.01, Gaussian Inc: Wallingford, CT, USA; 2010.
13. Schlegel HB. Optimization of equilibrium geometries and transition structures. *J. Comput. Chem.* 1982;3(2):214-218.
14. Ditchfield R, Hehre WJ, Pople JA. Self-consistent molecular orbital methods. xi. molecular orbital theory of nmr chemical shifts. *J. Chem. Phys.* 1971;54(10):4186-4193.
15. Dennington R, Keith T, Millam J. GaussView Version 5, Semichem Inc, Shawnee Mission, KS; 2009.
16. Becke AD. Density-functional thermochemistry. III. The role of exact exchange. *J Chem Phys.* 1993;98:5648-5652.
17. Koopmans T. Über die zuordnung von wellenfunktionen und eigenwerten zu den einzelnen elektronen eines atoms. *Physica.* 1993;1(1-6):104-113.
18. Lamère JF, Malfant I, Sourmia-Saquet A, Lacroix PG, Fabre JM, Kaboub L, Abbaz T, Gouasmia AK, Asselberghs I, Clays K. Quadratic nonlinear optical response in partially charged donor-substituted tetrathiafulvalene: From a computational investigation to a rational synthetic feasibility. *Chem Mater.* 2007;19(4):805-815.
19. Alorta I, Perez JJ. Molecular polarization potential maps of the nucleic acid bases. *Int. J. Quant. Chem.* 1996;57(1):123-135.
20. Scrocco E, Tomasi J. *Advances in quantum chemistry.* Academic Press, New York; 1978.
21. Luque FJ, Orozco M, Bhadane PK, Gadre SR. SCRF calculation of the effect of water on the topology of the molecular electrostatic potential. *J Phys Chem.* 1993;97(37):9380-9384.
22. Sethi A, Prakash R. Novel synthetic ester of Brassicasterol, DFT investigation including NBO, NLO response, reactivity descriptor and its intramolecular interactions analyzed by AIM theory. *J. Mol. Struct.* 2015;1083:72-81.
23. Gece G. The use of quantum chemical methods in corrosion inhibitor studies. *Corros Sci.* 2008;50(11):2981-2992.
24. Lewis DFV, Ioannides C, Parke DV. Interaction of a series of nitriles with the alcohol-inducible isoform of P450: Computer analysis of structure-activity relationships. *Xenobiotica.* 1994;24(5):401-408.
25. Uesugi Y, Mizuno M, Shimojima A, Takahashi H. Transient resonance raman and ab initio mo calculation studies of the structures and vibrational assignments of the t1 state and the anion radical of coumarin and its isotopically substituted analogues. *J Phys Chem.* 1997;101(3):268-274.
26. Padmaja L, Kumar CR, Sajjan D, Joe IH, Jayakumar V, Pettit GR. Density functional study on the structural conformations and intramolecular charge transfer from the vibrational spectra of the anticancer drug combretastatin-A2. *Journal of Raman Spectroscopy.* 2009;40(4):419-428.
27. Sudha S, Sundaraganesan N, Kurt M, Cinar M, Karabacak M. FT-IR and FT-Raman spectra, vibrational assignments, NBO analysis and DFT calculations of 2-amino-4-chlorobenzonitrile. *Journal of Molecular Structure.* 2011;985(2-3):148-156.
28. Fleming I. *Frontier orbitals and organic chemical reactions.* Wiley, London. 1976;27.
29. Fukui K. Role of frontier orbitals in chemical reactions. *Science.* 1982;218:747-754.
30. Parr RG, Szentpaly LV, Liu S. Electrophilicity index. *J Am. Chem. Soc.* 1999;121(9):1922-1924.
31. Parr RG, Chattaraj PK. Principle of maximum hardness. *J. Am. Chem. Soc.* 1991;113(5):1854-1855.

© 2016 Bendjeddou et al.; This is an Open Access article distributed under the terms of the Creative Commons Attribution License (<http://creativecommons.org/licenses/by/4.0>), which permits unrestricted use, distribution, and reproduction in any medium, provided the original work is properly cited.

*Peer-review history:*

*The peer review history for this paper can be accessed here:*  
<http://sciedomain.org/review-history/15084>